Nonclassical Ly6C(-) Monocytes Drive the Development of Inflammatory Arthritis in Mice

Misharin, Alexander V; Cuda, Carla M; Saber, Rana; Turner, Jason D; Gierut, Angelica K; Haines, G Kenneth; Berdnikovs, Sergejs; Filer, Andrew; Clark, Andrew R.; Buckley, Christopher D; Mutlu, Gökhan M; Budinger, G R Scott; Perlman, Harris

DOI:
10.1016/j.celrep.2014.09.032

Article

Cell Reports

Nonclassical Ly6C$^-$ Monocytes Drive the Development of Inflammatory Arthritis in Mice

Graphical Abstract

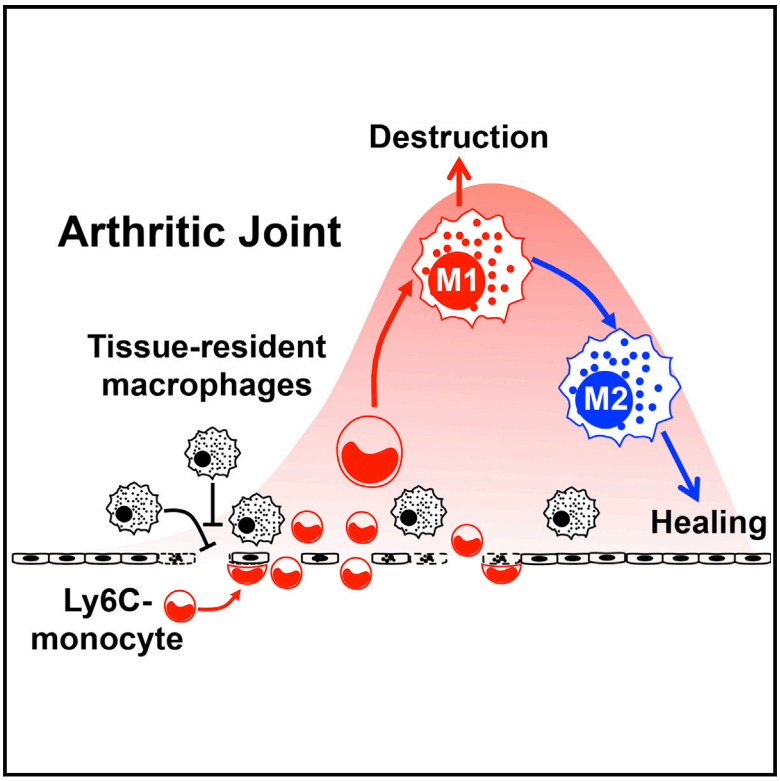

Highlights

Ly6C$^-$, but not Ly6C$^+$, monocytes are crucial for initiation of arthritis

Ly6C$^-$ monocytes give rise to inflammatory macrophages during arthritis

Tissue-resident synovial macrophages limit development of arthritis

Recruited macrophages change phenotype from M1 to M2 in situ

Authors

Alexander V. Misharin, Carla M. Cuda, ..., G.R. Scott Budinger, Harris Perlman

Correspondence

h-perlman@northwestern.edu

In Brief

Classical Ly6C$^+$ monocytes have been identified as important players in various inflammatory conditions; however, little is known about the role of the nonclassical Ly6C$^-$ monocytes. Here, Misharin et al. report that nonclassical Ly6C$^-$ monocytes are crucial for the initiation of joint inflammation in a mouse model of rheumatoid arthritis. This study also unveils phenotypical and ontological heterogeneity of the synovial macrophages in steady state and arthritis and reveals how macrophage polarization controls progression and resolution of the disease.

Misharin et al., 2014, Cell Reports 9, 591–604
October 23, 2014 ©2014 The Authors
http://dx.doi.org/10.1016/j.celrep.2014.09.032

Cell Reports
Article

Nonclassical Ly6C$^-$ Monocytes Drive the Development of Inflammatory Arthritis in Mice

Alexander V. Misharin,[1] Carla M. Cuda,[1] Rana Saber,[1] Jason D. Turner,[2] Angelica K. Gierut,[1] G. Kenneth Haines III,[3] Sergejs Berdnikovs,[4] Andrew Filer,[2] Andrew R. Clark,[2] Christopher D. Buckley,[2] Gökhan M. Mutlu,[5] G.R. Scott Budinger,[6] and Harris Perlman[1,*]

[1]Division of Rheumatology, Feinberg School of Medicine, Northwestern University, Chicago, IL 60611, USA
[2]Rheumatology Research Group, College of Medical and Dental Sciences, The University of Birmingham, Birmingham B15 2TT, UK
[3]Department of Pathology, Yale University, School of Medicine, New Haven, CT 06520, USA
[4]Division of Allergy and Immunology, Feinberg School of Medicine, Northwestern University, Chicago, IL 60611, USA
[5]Section of Pulmonary and Critical Care, Department of Medicine, University of Chicago, Chicago, IL 60637, USA
[6]Division of Pulmonary and Critical Care, Feinberg School of Medicine, Northwestern University, Chicago, IL 60611, USA
*Correspondence: h-perlman@northwestern.edu
http://dx.doi.org/10.1016/j.celrep.2014.09.032

SUMMARY

Different subsets and/or polarized phenotypes of monocytes and macrophages may play distinct roles during the development and resolution of inflammation. Here, we demonstrate in a murine model of rheumatoid arthritis that nonclassical Ly6C$^-$ monocytes are required for the initiation and progression of sterile joint inflammation. Moreover, nonclassical Ly6C$^-$ monocytes differentiate into inflammatory macrophages (M1), which drive disease pathogenesis and display plasticity during the resolution phase. During the development of arthritis, these cells polarize toward an alternatively activated phenotype (M2), promoting the resolution of joint inflammation. The influx of Ly6C$^-$ monocytes and their subsequent classical and then alternative activation occurs without changes in synovial tissue-resident macrophages, which express markers of M2 polarization throughout the course of the arthritis and attenuate joint inflammation during the initiation phase. These data suggest that circulating Ly6C$^-$ monocytes recruited to the joint upon injury orchestrate the development and resolution of autoimmune joint inflammation.

INTRODUCTION

Our understanding of the mononuclear phagocyte system in the initiation and resolution of inflammation has been significantly revised over the past years, in part due to discovery of heterogeneity of peripheral blood monocytes and tissue macrophages (Davies et al., 2013a; Ginhoux and Jung, 2014). Peripheral blood monocytes are subclassified into three different populations based on expression of cell-surface molecules and functions (Ziegler-Heitbrock et al., 2010). In humans, these populations correspond to CD14^{++}CD16$^-$ (classical monocytes), CD14^{++}CD16$^+$ (intermediate monocytes), and CD14$^+$CD16^{++} (nonclassical monocytes), and in mice, the equivalent populations are Ly6C$^+$CD62L$^+$CD43$^-$CCR2$^+$ (classical monocytes), Ly6C^{int}CD62L$^-$CD43$^+$CCR2$^-$ (intermediate monocytes), and Ly6C$^-$CD62L$^-$CD43$^+$CCR2$^-$ (nonclassical monocytes). An emerging literature suggests a previously unrecognized role for nonclassical Ly6C$^-$ monocytes during tissue injury. These cells patrol the luminal side of the endothelium and extravasate in response to both septic and aseptic tissue injury (Auffray et al., 2007), and recent work suggests that these cells may serve as precursors for alternatively activated macrophages (Auffray et al., 2009; Nahrendorf et al., 2007), playing a protective or anti-inflammatory role during tissue injury (Hamers et al., 2012; Hanna et al., 2012). However, the relative contribution of classical Ly6C$^+$ compared with nonclassical Ly6C$^-$ monocytes to tissue injury and repair is incompletely understood.

Another major component of the mononuclear phagocyte system is represented by tissue-resident macrophages. Classic work by van Furth identified bone-marrow-derived monocytes as precursors to tissue macrophages (van Furth and Cohn, 1968). However, recent studies showed that many tissue macrophages such as microglia in the brain, peritoneal macrophages, and Kupffer cells in the liver, originate from yolk sac or fetal liver progenitors (Ginhoux et al., 2010; Schulz et al., 2012; Yona et al., 2013). These tissue-resident macrophages are long lived and self-renewing via in situ proliferation, even in the absence of recruitment of circulating monocytes (Davies et al., 2011; Hashimoto et al., 2013; Jenkins et al., 2011), and have a gene-expression profile specific to their anatomical localization and microenvironment (Gautier et al., 2012). In adult animals, the macrophage population in the lung, peritoneal cavity, and spleen is more heterogeneous, with the addition of bone-marrow-derived macrophages during steady-state and inflammatory conditions (Davies et al., 2013b; Yona et al., 2013). The pro- and anti-inflammatory properties of tissue-resident macrophages have been primarily studied as a single population in the context of inflammation caused by microbes or parasites (Cailhier et al., 2006; Davies et al., 2011; Jenkins et al., 2011;

Maus et al., 2002). Moreover, the roles of tissue-resident macrophages during sterile inflammation are unknown and the relative contributions of tissue-resident or monocyte-derived macrophages in any models of inflammation are largely unexplored.

Both tissue-resident and bone-marrow-derived macrophages exhibit significant functional heterogeneity and may differentiate or be polarized into one of two main macrophage subtypes: classically activated, M1 (proinflammatory), and alternatively activated, M2 (anti-inflammatory/resolution phase), macrophages (Lech and Anders, 2013; Sica and Mantovani, 2012). Whereas some studies suggest that alternatively, anti-inflammatory macrophages may originate from a new wave of monocytes entering into tissues during the resolution of inflammation (Nahrendorf et al., 2007; Shechter et al., 2009, 2013), it is still not known if, during disease pathogenesis, bone-marrow-derived classically activated macrophages can exhibit plasticity and switch their phenotype toward an alternatively activated one in situ.

Rheumatoid arthritis (RA) is a chronic autoimmune disease affecting up to 1% of the world's population (Helmick et al., 2008), which makes it one of the most prevalent autoimmune conditions. During RA, the dysregulation of the immune system leads to destruction and deformation of the joint, resulting in chronic pain, severe disability, and increased mortality. Circulating monocytes in patients with RA are known to be activated (Kawanaka et al., 2002; Kinne et al., 2007; Stuhlmüller et al., 2000; Torsteinsdóttir et al., 1999), and the number of macrophages in the synovium correlates with joint damage (Mulherin et al., 1996) and clinical response to therapy (Haringman et al., 2005). Murine models of RA represent a clinically relevant system for deciphering the role of monocytes and macrophages in the pathogenesis of sterile chronic autoimmune inflammation (Vincent et al., 2012).

Here, we used a mouse model of immune-complex, sterile, inflammatory arthritis to uncover novel roles for monocyte subsets and macrophages during distinct phases of disease development. We demonstrate that circulating Ly6C$^-$ monocytes are recruited to the joint during the effector phase of arthritis and differentiate into classically activated macrophages, which drive the development of the joint pathology. However, as the arthritis progresses, these same classically activated macrophages change from a classically to an alternatively activated phenotype, which is necessary for the resolution of joint inflammation. This remarkable influx of Ly6C$^-$ monocytes and their dramatic changes in polarization occurred without significant changes in the number or phenotype of tissue-resident synovial macrophages. These findings suggest a new paradigm for understanding the pathogenesis of RA, in which nonclassical monocytes recruited to the joint exhibit remarkable phenotypic plasticity over the course of arthritis, promoting first tissue injury and then repair, overwhelming the constitutive anti-inflammatory effects of the tissue-resident macrophages.

RESULTS

Differential Role of Monocyte Subsets in the Initiation of Inflammatory Arthritis

The temporal changes in monocyte populations in murine models of autoimmune arthritis and their contribution to important disease phenotypes are still unknown. Here, we used a murine model of sterile inflammatory arthritis (K/BxN serum-*t*ransfer-*i*nduced *a*rthritis [STIA]), which models the effector phase of human RA; is independent of the adaptive immune response; and consists of initiation, propagation, and resolution phases (Monach et al., 2008). To deplete monocytes, we injected clodronate-loaded liposomes intravenously 24 hr prior to the induction of arthritis. Virtually all monocytes in the peripheral blood and the red pulp macrophages in spleen were depleted for 48–72 hr following the clodronate-loaded liposome treatment, whereas the number of circulating neutrophils and synovial macrophages was unchanged (Figure S1A). Monocyte depletion completely prevented the development of STIA (Figure 1A) and suppressed the recruitment of neutrophils to the joints (Figure S1B). Additionally, treatment with clodronate-loaded liposomes at days 3 and 5 of STIA led to an abrupt end to the development of STIA (Figure 1B). Because recent studies suggested that the splenic pool of monocytes may also contribute to acute inflammation, we splenectomized mice and showed that there was no difference in ankle swelling or clinical scores between the groups following the induction of STIA (Figure S1C).

To address the contribution of Ly6C$^+$ monocytes to the initiation and development of STIA, we depleted classical Ly6C$^+$ monocytes using anti-CCR2 antibody. Whereas Ly6C$^+$ monocytes were dramatically reduced in the peripheral blood and spleen following injection of anti-CCR2 antibody (Figure S1D), the induction and development of STIA occurred normally (Figure S1E). Similarly, *CCR2*$^{-/-}$ mice, which lack CCR2 on both classical and nonclassical monocytes, were able to develop STIA and recruit both neutrophils and macrophages into the joint (Figure S1F).

Because tools for selective depletion of nonclassical Ly6C$^-$ monocytes are not available, we developed approaches to investigate the role of this population in the initiation of STIA. First, we depleted monocytes using clodronate-loaded liposomes, and STIA was induced at different stages of monocyte subset recovery. Whereas nonclassical Ly6C$^-$ monocytes failed to recover even 7 days after injection of clodronate-loaded liposomes, the total number of monocytes and neutrophils were similar to controls at 7 days following the injection of clodronate-loaded liposomes (Figures 1C and S1G). The absence of Ly6C$^-$ monocytes was also associated with an inability to develop STIA (Figure 1D). Next, we treated mice with clodronate-loaded liposomes 2 days prior to the initiation of arthritis, and classical Ly6C$^+$ or nonclassical Ly6C$^-$ monocytes isolated from bone marrow were adoptively transferred immediately after initiation of STIA. Mice that received Ly6C$^-$ monocytes developed STIA at the same rate as control-treated animals (Figure 1E); however, mice that received Ly6C$^+$ monocytes exhibited a marked delay in the development of STIA. These results likely reflect the conversion of classical Ly6C$^+$ monocytes into nonclassical Ly6C$^-$ monocytes after adoptive transfer (Yona et al., 2013) or recovery of the depleted monocyte pool.

The Normal Adult Mouse Joint Contains Heterogeneous Population of Tissue-Resident Macrophages

To further explore the role of Ly6C$^-$ nonclassical monocyte subsets in the development of inflammatory arthritis, we first

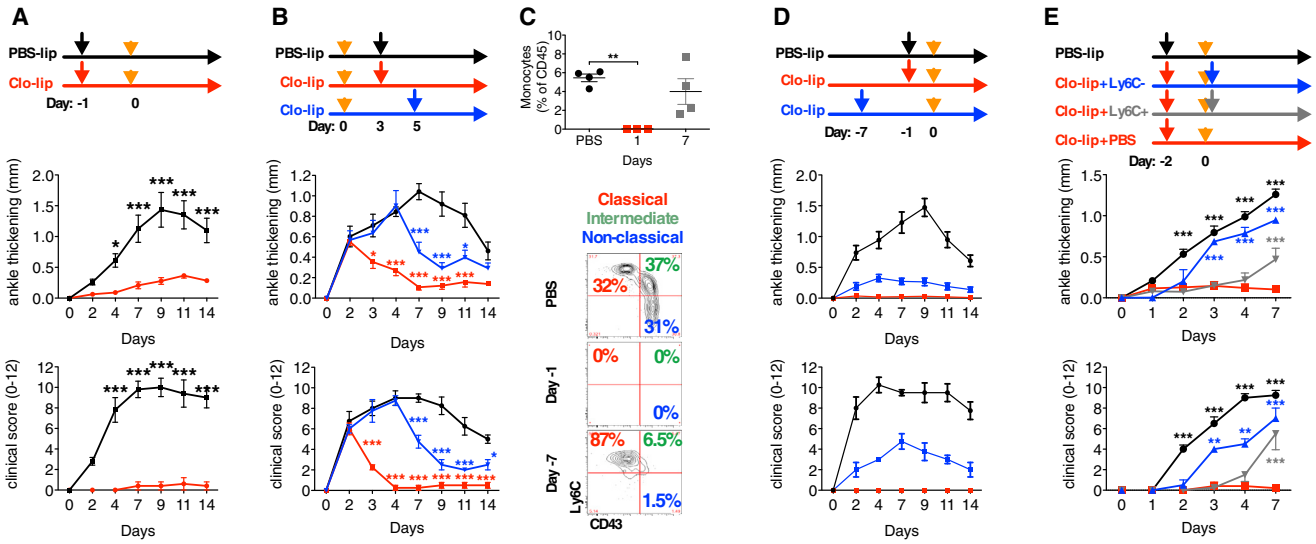

Figure 1. Role of Monocytes in the Initiation and Development of STIA

(A) Depletion of monocytes using clodronate-loaded liposomes prevents initiation and development of STIA (n = 5). Orange arrows indicate injection of K/BxN serum; black and red—PBS and clodronate-loaded liposomes, correspondingly.

(B) Depletion of monocytes during development of STIA (n = 4) leads to its abrupt ending. Mice were treated with clodronate-loaded liposomes at indicated time points. Orange arrows indicate injection of K/BxN serum; black, blue, and red—PBS and clodronate-loaded liposomes, correspondingly.

(C and D) Absence of Ly6C$^-$ monocytes prevents STIA. Monocytes were depleted using clodronate-loaded liposomes. (C) Representative contour plots gated on CD45$^+$CD115$^+$CD11b$^+$ blood cells (numbers represent percentages of the parent population). (D) Representative arthritis scores (n = 4).

(E) Adoptive transfer of Ly6C$^-$ monocytes restores STIA. Monocytes were depleted with clodronate-loaded liposomes (red arrows) and 48 hr later 1 × 10^6 classical Ly6C$^+$ (n = 4; gray arrow) or 0.5 × 10^6 nonclassical Ly6C$^-$ (n = 2; blue arrow) monocytes sorted from bone marrow or PBS (control) were transferred via intravenous injection, immediately following injection of K/BxN serum (orange arrows) to induce STIA. Another cohort of control mice was treated with PBS-loaded liposomes (n = 4; black arrow).

All data are represented as mean ± SEM. Differences between groups were compared using two-way ANOVA for repeated measurements with Bonferroni posttest; *p < 0.05; **p < 0.01; ***p < 0.001.

examined the cellular composition of the murine joint in unchallenged, normal wild-type mice using multiparameter flow cytometry (Figure 2A). After excluding doublets, dead cells, and nonhematopoietic cells, we identified myeloid cells as CD11b$^+$ and then excluded eosinophils (Siglec F$^+$), neutrophils (Ly6G$^+$), and CD11b$^+$ dendritic cells (DCs) (CD11b$^+$CD11c^{high} MHC II$^+$CD64$^-$). We then subdivided the remaining CD11b$^+$ cells into Ly6C$^+$CD11b$^+$CD11c$^-$F4/80^{low}CD64^{int} cells (referred as Ly6C$^+$CD64^{int} cells) and CD11b$^+$CD11c^{int}F4/80$^+$CD64$^+$ cells (macrophages). We further subclassified the macrophage population as major histocompatibility complex (MHC) II$^+$ or MHC II$^-$, with the majority being MHC II$^-$ macrophages (80%–85%). Cytospin analysis (Figure 2B) revealed that MHC II$^-$ macrophages were smaller (10.0 ± 1.8 μM versus 8.9 ± 1.8 μM, correspondingly) and had more condensed chromatin in the nuclei and more granular cytoplasm as compared to MHC II$^+$ macrophages, which had brighter nuclei and large vacuoles in the cytoplasm. Additionally, both populations of macrophages had similar surface expression of classic macrophage markers, receptors involved in phagocytosis, and uptake of apoptotic bodies with the exception of Tim-4 and CX_3CR1 (Figure S2A). Immunofluorescent microscopy confirmed that the MHC II$^+$ and MHC II$^-$ macrophages were located within the synovial lining (Figure S2B). Further, human synovial CD68+ macrophages obtained from synovial biopsies in healthy volunteers or patients with RA were also heterogeneous with respect to HLA-DR and CD163 expression (Figure S2C).

To define the contribution of bone-marrow-derived monocytes to the persistence of Ly6C$^+$CD64^{int} cells and MHC II$^-$ and MHC II$^+$ synovial macrophages, we generated bone marrow chimeras by irradiating CD45.1 hosts and transferring CD45.2 bone marrow cells. Almost 80% of the MHC II$^-$ synovial macrophages were recipient origin even 2 months posttransfer (Figure 2C). These data suggest that this population was radioresistant and long lived and does not require a contribution from circulating monocytes. In contrast, Ly6C$^+$CD64^{int} cells and MHC II$^+$ macrophages were rapidly replaced by donor cells, similar to other bone-marrow-derived macrophages, such as pulmonary interstitial macrophages, small peritoneal macrophages, and splenic monocytes (Figure S2D). We then analyzed ankles from *CCR2*$^{-/-}$ mice, which have a decreased number of monocytes in the circulation. In agreement with the bone marrow chimera data, *CCR2*$^{-/-}$ mice had reduced numbers of Ly6C$^+$CD64^{int} cells, CD11b$^+$ DC, and MHC II$^+$ macrophages, whereas the numbers of MHC II$^-$ macrophages were not affected (Figure S2E). The number of synovial MHC II$^-$, but not MHC II$^+$, macrophages was dramatically decreased in the ankle joint (Figure 2D) from mice that lack macrophage colony stimulating factor (M-CSF) (*Csf1*^{op}/*Csf1*^{op}). Because previous studies have suggested that M-CSF-responsive macrophages are derived from the yolk sac or fetal progenitors (Ginhoux et al., 2010; Ginhoux and Jung,

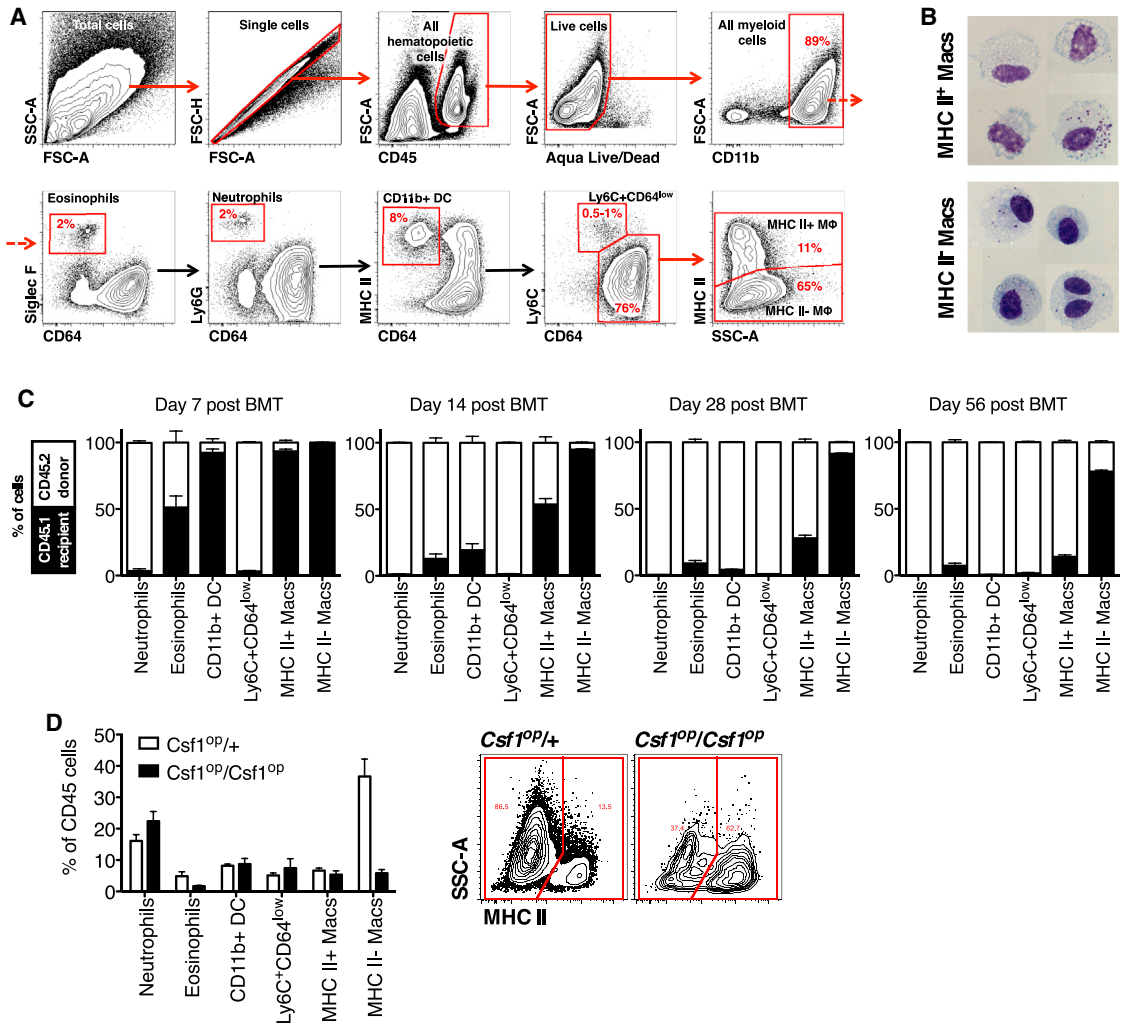

Figure 2. Characterization of Synovial Macrophages under Steady-State Conditions in the Mouse Joint

(A) Flow cytometry analysis of a mouse joint during steady-state conditions. Numbers on the contour plots represent percentages of CD45$^+$ cells.

(B) Photomicrographs of sorted MHC II$^+$ and MHC II$^-$ macrophages. The scale bar represents 5 μm.

(C) MHC II$^-$ macrophages exhibit radioresistance and do not require input from bone marrow. Bone marrow transfer (n = 4 per time point) was performed as described in the Experimental Procedures.

(D) Left: number of MHC II$^-$ macrophages was dramatically reduced in the synovium of Cfs1$^{op/op}$ mice (n = 4). Right: representative contour plots showing decrease of MHC II$^-$ macrophages in the synovium. Numbers on the contour plots represent percentages of the parent population (macrophages).

2014; Lichanska et al., 1999), these data suggest that, under steady-state conditions, majority MHC II$^-$ macrophages represent true tissue-resident macrophages, whereas most of the MHC II$^+$ synovial macrophages originate from bone marrow. Furthermore, as the host's Ly6C$^+$CD64^{int} cells were completely replaced in the bone marrow chimeras, decreased in *CCR2*$^{-/-}$ mice, and unaffected by the intravenous injection of clodronate-loaded liposomes in wild-type (WT) mice, the Ly6C$^+$CD64^{int} cells likely represent classical Ly6C$^+$ monocytes, which extravasated into tissues for surveillance (Jakubzick et al., 2013).

Peripheral Blood Monocytes Give Rise to Recruited Macrophages during STIA

To better understand the contribution of monocytes throughout the initiation, sustainment, and remission phases of STIA, we analyzed the cellular composition of mouse ankles during the course of STIA. All populations of myeloid cells expanded during the initiation and propagation phases of STIA (Figure 3A). Neutrophils were the predominant cell subset during the peak of STIA; however, their number rapidly declined during the resolution phase. Macrophage populations also changed over the course of STIA. The MHC II$^+$ subset prevailed during the propagation phase, whereas the MHC II$^-$ subset became the predominant cell type during the resolution phase (Figure 3A). We then focused on the early events of STIA (Figure S3A) and found an increase in the number of MHC II$^+$ macrophages first evident at day 2 followed by an increase in the number of neutrophils at day 3. These data indicate that the influx of monocytes and their differentiation into macrophages precedes the recruitment of neutrophils.

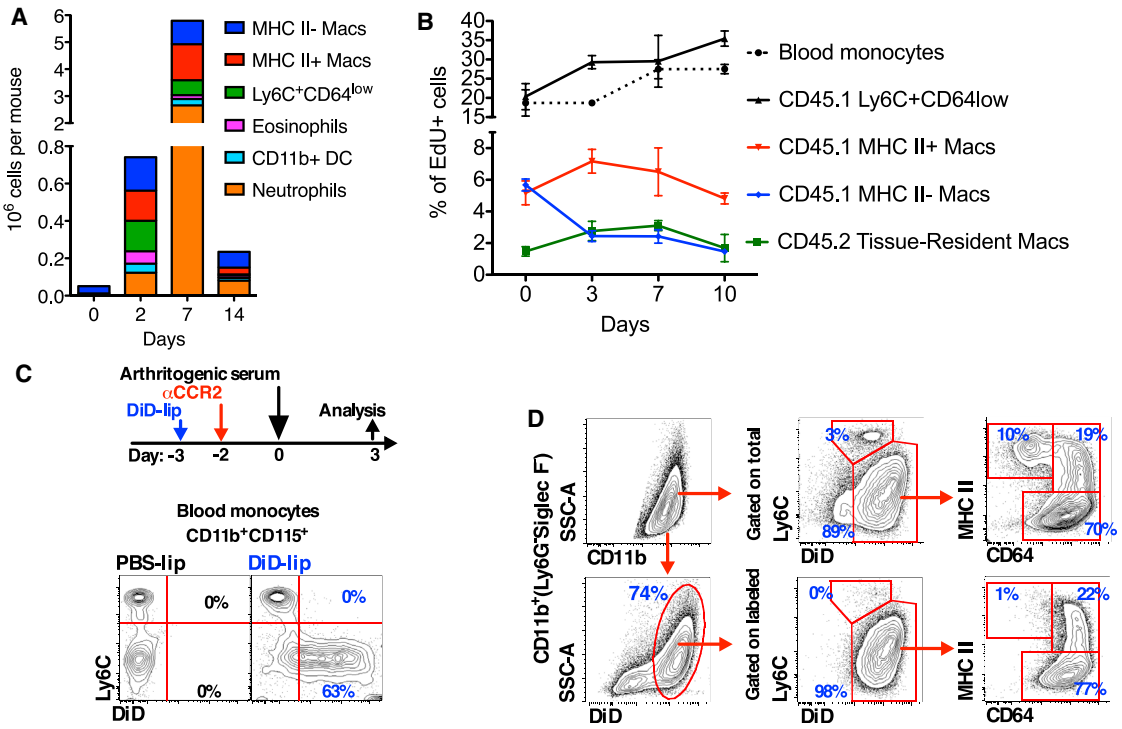

Figure 3. Origin of Inflammatory Macrophages in the Arthritic Joint

(A) Dynamics of the individual cell subsets in the synovium during the course of STIA (n = 4).

(B) Analysis of EdU incorporation during the course of STIA. Arthritis was induced in bone marrow chimeras with shielded ankles as described in the Supplemental Experimental Procedures section.

(C) Nonclassical Ly6C$^-$ monocytes were labeled as described in the Experimental Procedures section. Representative contour plots are shown and numbers represent percentages of monocytes.

(D) Nonclassical Ly6C$^-$ monocytes are recruited to the arthritic joint and give rise to both MHC II$^+$ and MHC II$^-$ macrophages. Data are represented as mean ± SEM.

To unravel the relationships between the monocyte/macrophage subsets in the arthritic joint (blood monocytes, tissue-resident macrophages, and inflammatory macrophages), we performed a series of cell-labeling studies. To discriminate between tissue-resident (CD45.2) and recruited cells (CD45.1), we generated bone marrow chimeras (CD45.1 → CD45.2), but this time, the ankles were shielded during irradiation (see Supplemental Experimental Procedures). Mice were then pulsed with a single injection of 5-ethynyl-2′-deoxyuridine (EdU) during different stages of STIA (D-1, D2, D6, and D9), and incorporation of EdU into donor cells (CD45.1) and host tissue-resident macrophages (CD45.2) was analyzed 24 hr later (D0, D3, D7, and D10; Figure 3B). Within this time frame, only classical Ly6C$^+$ monocytes were labeled in peripheral blood (Figure S3B). The percentage of EdU$^+$Ly6C$^+$CD64^{int} cells (CD45.1) was similar to circulating monocytes (CD45.1; Figure 3B). The percent of EdU$^+$ MHC II$^+$ bone-marrow-derived macrophages (CD45.1) was higher compared to EdU$^+$ MHC II$^-$ macrophages (Figure 3B). After 48 hr (D2 of STIA), the percent EdU$^+$ donor monocytes (CD45.1) and Ly6C$^+$CD64^{int} CD45.1 cells decreased, whereas the percent of EdU+ bone-marrow-derived macrophages (CD45.1) reciprocally increased (Figure S3C). We then investigated whether local proliferation of tissue-resident macrophages contributes to the increased number of macrophages during STIA. Tissue-resident macrophages (CD45.2) exhibited low levels of proliferation in the steady state (D0; 1.47% ± 0.51%), which increased during the peak of arthritis (day 7; 3.10% ± 0.54%; p = 0.0198) and returned to baseline during the resolution of STIA (day 10; 1.68% ± 1.49%; p = 0.82). However, despite their ability to proliferate, the total number of tissue-resident macrophages (CD45.2) did not change during the course of STIA. Moreover, the ratio of recruited macrophages to tissue-resident macrophages ranged between 7:1 and 20:1 during STIA (Figure S3D). Taken together, these data suggest that monocyte recruitment and not local proliferation of tissue-resident macrophages contributes to increased number of macrophages during STIA and that the overwhelming majority of macrophages in the joint are derived from monocytes that extravasate during STIA.

Nonclassical Ly6C$^-$ Monocytes Preferentially Give Rise to MHC II$^-$ Macrophages during STIA

Because our data indicate that nonclassical Ly6C$^-$ monocytes are required for STIA (Figures 1C and 1D), we examined whether they are recruited into arthritic joint. We labeled Ly6C$^-$ monocytes (Figure 3C) and tracked their fate upon induction of STIA (Figure 3D). There were no labeled Ly6C$^-$ monocytes in the joint in the nonarthritic mouse 3 days postlabeling (T = 0). In contrast, the labeled Ly6C$^-$ monocytes entered into arthritic joint and

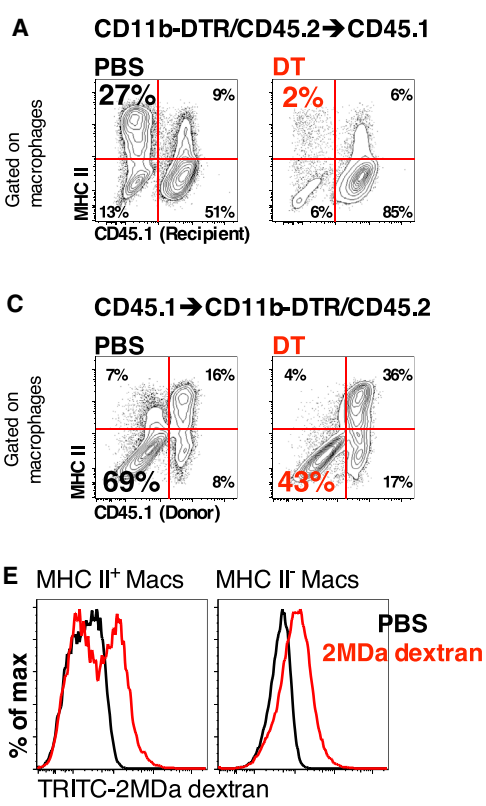

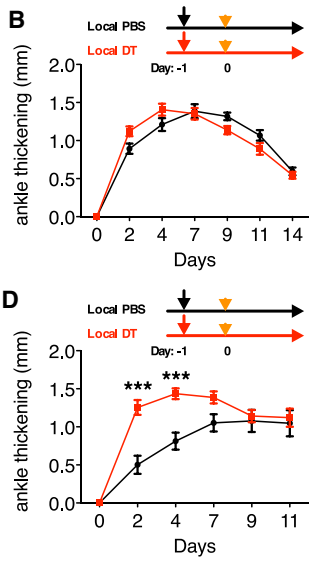

Figure 4. Role of Tissue-Resident Macrophages in the Initiation of STIA

(A) Local injection of DT depletes donor-derived macrophages in CD11b-DTR→CD45.1 bone marrow chimeric mice. Representative contour plots gated on macrophages are shown (numbers indicate percentages of the parent population).

(B) Depletion of MHC II$^+$ macrophages does not affect initiation and development of STIA (n = 5).

(C) Local injection of DT depletes host macrophages in CD45.1→CD11b-DTR bone marrow chimeric mice and does not affect donor-derived macrophages. Representative contour plots gated on macrophages are shown (numbers indicate percentages of the parent population).

(D) Depletion of MHC II$^-$ macrophages accelerate development of STIA (n = 10). Data are represented as mean ± SEM. Differences between groups were compared using two-way ANOVA for repeated measurements with Bonferroni posttest; *p < 0.05; **p < 0.01; ***p < 0.001.

(E) Phagocytosis of high-molecular-weight TRITC-labeled dextran by subpopulations of myeloid cells in the naive mouse joint. Representative histograms are shown.

developed into both MHC II$^-$ (77%) and MHC II$^+$ (22%) synovial macrophages during STIA (Figure 3D). These data indicate that nonclassical Ly6C$^-$ monocytes give rise to inflammatory macrophages in the context of STIA. To determine fate of synovial macrophages during STIA, we adoptively transferred MHC II$^+$ and MHC II$^-$ synovial macrophages sorted from ankles of day 3 STIA *Cx3cr1*$^{gfp/+}$ mice into the periarticular space of day 3 STIA CD45.1 mice (Figures S3E and S3F). Synovial macrophages exhibited plasticity in terms of MHC II expression, as 50% of transferred MHC II$^+$ macrophages became MHC II$^-$ and almost 25% of transferred MHC II$^-$ macrophages were MHC II$^+$ between days 3 and 10 of STIA. In contrast, when we sorted and adoptively transferred MHC II$^+$ and MHC II$^-$ macrophages from day 7 of STIA and followed them into the late-resolution phase (day 18), almost 100% of cells became MHC II$^-$ (Figures S3G and S3H).

Tissue-Resident Macrophages Attenuate the Severity of STIA

To understand the roles played by tissue-resident (MHC II$^-$) and bone-marrow-derived (MHC II$^+$) macrophages in the development of STIA, we selectively deleted these populations from the naive joint prior to the development of STIA. To accomplish this, we took advantage of the CD11b-diphtheria toxin receptor (DTR) system, in which monocytes and bone-marrow-derived macrophages express the DTR under the control of the CD11b promoter. We used these mice to create two groups of bone marrow chimeras: (1) CD11b-DTR bone marrow (CD11b-DTR/CD45.2) into lethally irradiated CD45.1 recipients (CD11b-DTR→CD45.1) and (2) by CD45.1 bone marrow into CD11b-DTR/CD45.2 recipients (CD45.1→CD11b-DTR). Consistent with the wild-type chimeras (Figure 2C), more than 80% of the tissue-resident MHC II$^-$ macrophages were of recipient origin, whereas the vast majority of the tissue-resident MHC II$^+$ macrophages were derived from the donor bone marrow (Figures 4A and 4C). We then treated CD11b-DTR→CD45.1 and CD45.1→CD11b-DTR mice with an intra-articular injection of low-dose diphtheria toxin (DT), which does not affect the circulating monocyte pool (Figure S4A), and then induced STIA 24 hr later. Loss of MHC II$^+$ macrophages in CD11b-DTR→CD45.1 mice had no effect (Figure 4B) on the course of STIA, whereas depletion of tissue-resident MHC II$^-$ macrophages in CD45.1→CD11b-DTR mice led to increased arthritis (Figure 4D). To explore how tissue-resident macrophages might attenuate joint inflammation during STIA, we examined their phagocytic capacity in vivo. All MHC II$^-$ macrophages phagocytized 2 MDa tetramethylrhodamine (TRITC)-labeled dextran, whereas only a portion (50%) of MHC II$^+$ macrophages were TRITC positive (Figure 4E). These data suggest that MHC II$^-$ tissue-resident macrophages play an important role in maintaining joint integrity and may limit the development of arthritis.

Recruited Monocytes and Inflammatory Macrophages Are Required for the Propagation Phase in STIA

We have shown that nonclassical Ly6C$^-$ monocytes are essential for the initiation and propagation of STIA and give rise to inflammatory macrophages. To investigate the role of these monocytes and bone-marrow-derived macrophages during the

effector phase of STIA, we depleted them by systemically administering DT to CD11b-DTR→CD45.1 chimeric mice. Peripheral blood monocytes and bone-marrow-derived synovial macrophages were depleted after systemic treatment with DT (Figures 5A and 5B), whereas host MHC II$^-$ tissue-resident macrophages (DTR$^-$) were insensitive to DT (Figure 5B). When we repeatedly treated CD11b-DTR→CD45.1 mice DT, the severity of arthritis as measured by ankle swelling and clinical scores was markedly decreased as compared to controls. The small amount of arthritis that developed in the CD11b-DTR→CD45.1 mice was associated with an increased number of neutrophils in the joint as compared to nonarthritic controls, but not macrophages (Figure 5D). Repeated administration of DT prevented the propagation phase (Figure 5D), which resulted in reduced histological scores of arthritis (Figures 5F and 5G). Additionally, the number of stromal (CD45$^-$) cells did not change throughout STIA (Figure 5E). To exclude a requirement for DCs in the development of STIA, we generated CD11c-DTR→CD45.1 chimeric mice and subjected them to repeated administration of DT. Despite the fact that CD11b$^+$ DCs were deleted (Figure S4B), DT-treated mice exhibited similar levels of arthritis as compared to control mice (Figure S4C).

Recruited Tissue Macrophages, but Not Blood Monocytes, Are Required for the Resolution of STIA

Recent findings suggest that resolution of sterile inflammation may require recruitment of monocytes into tissues (Nahrendorf et al., 2007; Soehnlein and Lindbom, 2010). However, when we depleted blood monocytes at the peak of arthritis using intravenous injection of clodronate-loaded liposomes, the resolution of arthritis was unchanged (Figure 6A). In contrast, when we depleted both blood monocytes and recruited macrophages using systemic treatment of chimeric CD11b-DTR→CD45.1 mice with DT at the peak of arthritis, the resolution of arthritis was delayed as evidenced by sustained elevations in the histopathological scores for pannus, cartilage destruction, and bone erosion relative to untreated mice (Figures 6B–6E).

Synovial Macrophages Are Reprogrammed from Inflammatory toward a Resolution Phenotype

Our data suggest that the same population of macrophages responsible for the development of arthritis also participated in its resolution. Macrophages may be polarized to a particular phenotype that is dependent on the environmental milieu; therefore, we examined whether synovial macrophages undergo a change in phenotype from classically activated M1 macrophages that drive destruction of the joint to alternatively activated M2 macrophages that are necessary for healing. Polarization of synovial macrophages in the naive joint (D0) during the peak of STIA (D7) and during the resolution phase of STIA (D14) was assessed on sorted MHC II$^+$ and MHC II$^-$ synovial macrophages, which were analyzed for gene expression using a custom QuantiGene 2.0 panel (Table S4). Among the 52 genes included into the panel, 46 were differentially expressed between macrophage subsets according to selected criteria (differentially expressed in at least one two-group comparison; false discovery rate [FDR]-corrected q-value < 0.001; Table S5). Principal component analysis revealed that MHC II$^-$ and MHC II$^+$ macrophages in the naive joint (D0) clustered separately from each other along PC2 axis, which is in agreement with differential origin of these populations (tissue-resident versus bone-marrow-derived; Figures 7A and 7B). Twenty-three genes were differentially expressed between MHC II$^+$ and MHC II$^-$ macrophages in the steady state (D0; Table S5), including *Timd4*, which is in agreement with data obtained via flow cytometry (Figure S2A). Further, the MHC II$^+$ and MHC II$^-$ macrophages recruited into the joint during STIA (D7 and D14) also clustered together. We then selectively compared the polarization profiles of synovial macrophages at the peak of STIA and during its resolution with MHC II$^+$ D0 macrophages, which are bone-marrow-derived and, therefore, more closely resemble macrophages recruited during STIA. At both the peak of STIA (day 7) and during the resolution of STIA (day 14), both MHC II$^+$ and MHC II$^-$ macrophages exhibited an enhanced M1 and intermediate M2 polarization profile compared with MHC II$^+$ macrophages at D0. These changes included increased expression of several M1 genes (*Nfkb1*, *Il1b*, *Cd80*, *Il12b*, and *Fcrg1*) and some M2 genes (*Pparg*, *Tnfsf14*, *Il1rn*, *Tgm2*, *Chi3l3*, and *Arg1*), with reduced expression of other M2 genes (*Timd4*, *Relma*, *Irf4*, *Cd36*, *Cxcl13*, *Ccl17*, *Shpk*, *Nr4a1*, and *Mrc1*). Interestingly, the expression of *Mertk*, which is involved in uptake of apoptotic cells, was increased in both MHC II$^+$ and MHC II$^-$ macrophages during the resolution of STIA, but not at its peak.

We then compared the gene expression of MHC II$^+$ and MHC II$^-$ macrophage populations at the peak (D7) of STIA. MHC II$^+$ macrophages expressed more M1-associated genes (*Il1b*, *Il12b*, *CD80*, and *CD86*) and some M2-associated genes (*Pparg*, *Il1rn*, *Kdm6b*, *Tnfsf14*, *Socs1*, *Il33*, and *Ccl17*) compared to MHC II$^-$ macrophages. However, the expression of several M2-associated genes was increased in the MHC II$^-$ compared with MHC II$^+$ macrophages including *Timd4*, *Tfrc*, *CD36*, *CD163*, *Cxcl13*, *Mertk*, and the hallmark gene of murine M2 activation—*Arg1*. The only M1 gene, which was expressed at higher levels in MHC II$^-$ macrophages, was *Tnf*. A similar pattern was observed during the resolution phase of STIA (D14). Day 14 MHC II$^+$ macrophages expressed more M1 (*Il1b*, *Il6*, *Il12b*, and *CD86*) and some M2 genes (*Retnla*, *Pparg*, *Il1rn*, *Kdm6b*, *Tnfsf14*, *Socs1*, *Il33*, *Ccl17*, *Irf4*, *Hbegf*, *Nr4a1*, *Il10*, and *Mrc1*) whereas MHC II$^-$ macrophages expressed higher levels of M2 genes (*Timd4*, *CD36*, *Cxcl13*, *Tgm2*, and *Arg1*). Taken together, these data suggest that both MHC II$^+$ and MHC II$^-$ macrophages exhibit mixed M1/M2 polarization during STIA. However, MHC II$^-$ macrophages express more M2 genes throughout the course of STIA. Because many of the genes differentially expressed in MHC II$^-$ macrophages are involved in uptake of apoptotic bodies and resolution of inflammation, we analyzed expression of CD36 (Figure 7C), a member of class B scavenger receptor family involved in the uptake of apoptotic bodies (efferocytosis) and a marker of alternatively activated macrophages (Xiong et al., 2013). In agreement with the gene-expression profiles, we found that only fraction MHC II$^+$ macrophages expressed CD36 during STIA, unlike MHC II$^-$ macrophages, which uniformly expressed high levels of CD36. Taken together, these data and the fate-mapping studies suggest that change in macrophage phenotype during STIA from MHC II$^+$ to MHC II$^-$ is associated with transition from M1 to M2 phenotype.

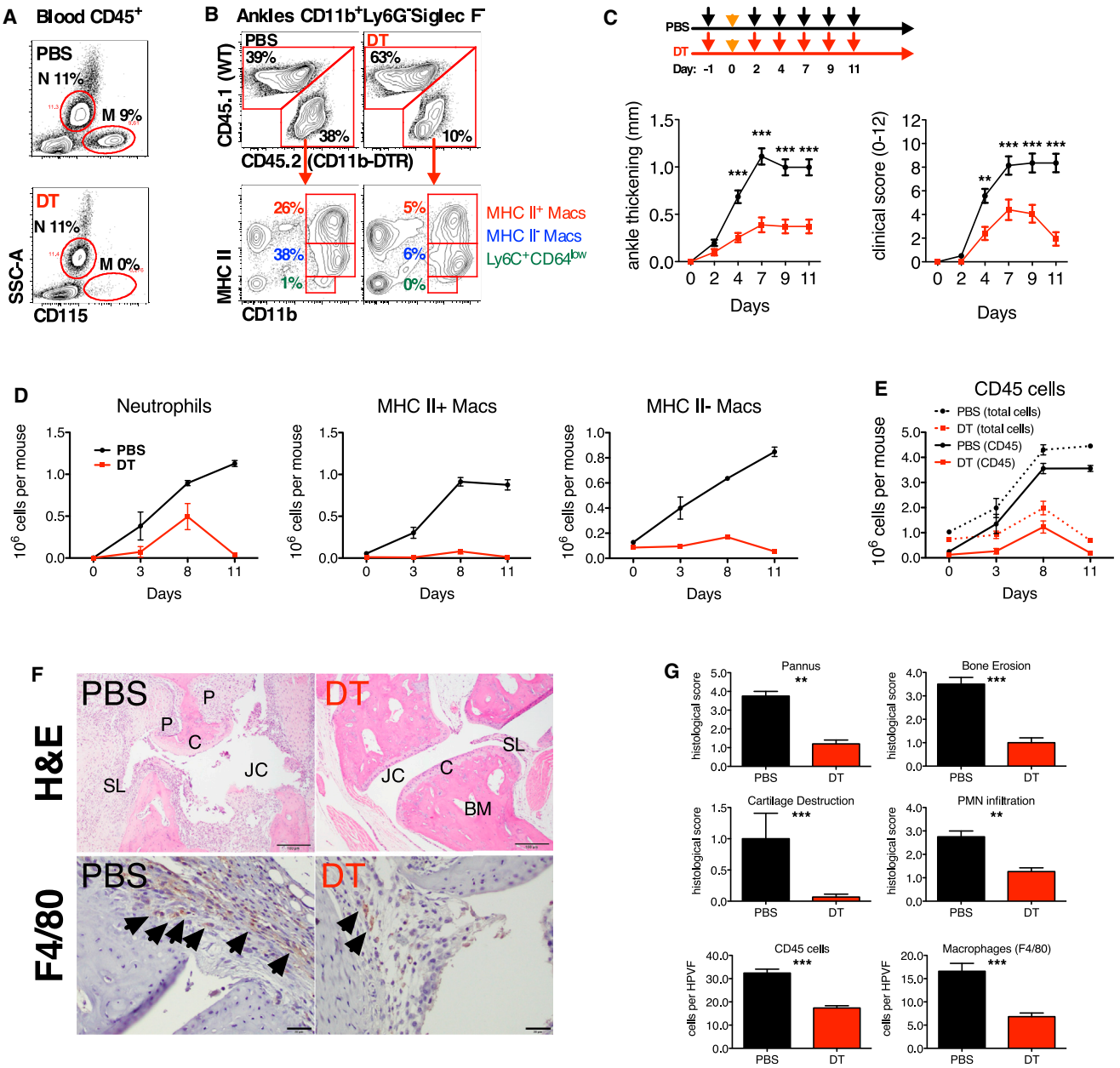

Figure 5. Recruitment of Monocytes and Differentiation into Macrophages Are Required for Development of Joint Pathology during STIA

(A) Systemic treatment with DT eliminated blood monocytes while sparing neutrophils. Representative contour plots are shown. Numbers represent percentages of $CD45^+$ cells.

(B) Systemic treatment with DT eliminates DTR-expressing tissue macrophages (CD45.2) in the synovium of CD11b-DTR(CD45.2)→CD45.1 bone marrow chimeras. Representative contour plots are shown, and numbers indicate percentages of $CD45^+$ cells.

(C) Repeated administration of DT decreases severity of arthritis (n = 10).

(D) Continuous treatment with DT decreased number of cells recruited to the joint (n = 4 per time point).

(E) Dynamic of myeloid cell subsets in the joints during the course of STIA in PBS and DT-treated mice.

(F) Depletion of tissue macrophages during effector phase of STIA decreases joint damage. Top: hematoxylin and eosin staining (tibiotalar joint is shown); scale bar represents 100 μm. BM, bone marrow; C, cartilage; H&E, hematoxylin and eosin; JC, joint cavity; P, pannus; SL, synovial lining. Bottom: immunohistochemical staining for macrophage marker F4/80. Arrows indicate F4/80-positive cells. The scale bar represents 20 μm.

(G) Depletion of tissue macrophages decreases histopathological scores. HPVF, high-power view field; PMN, polymorphonuclear neutrophil.

Data are represented as mean ± SEM. Differences between groups were compared using two-way ANOVA for repeated measurements with Bonferroni posttest; *p < 0.05; **p < 0.01; ***p < 0.001.

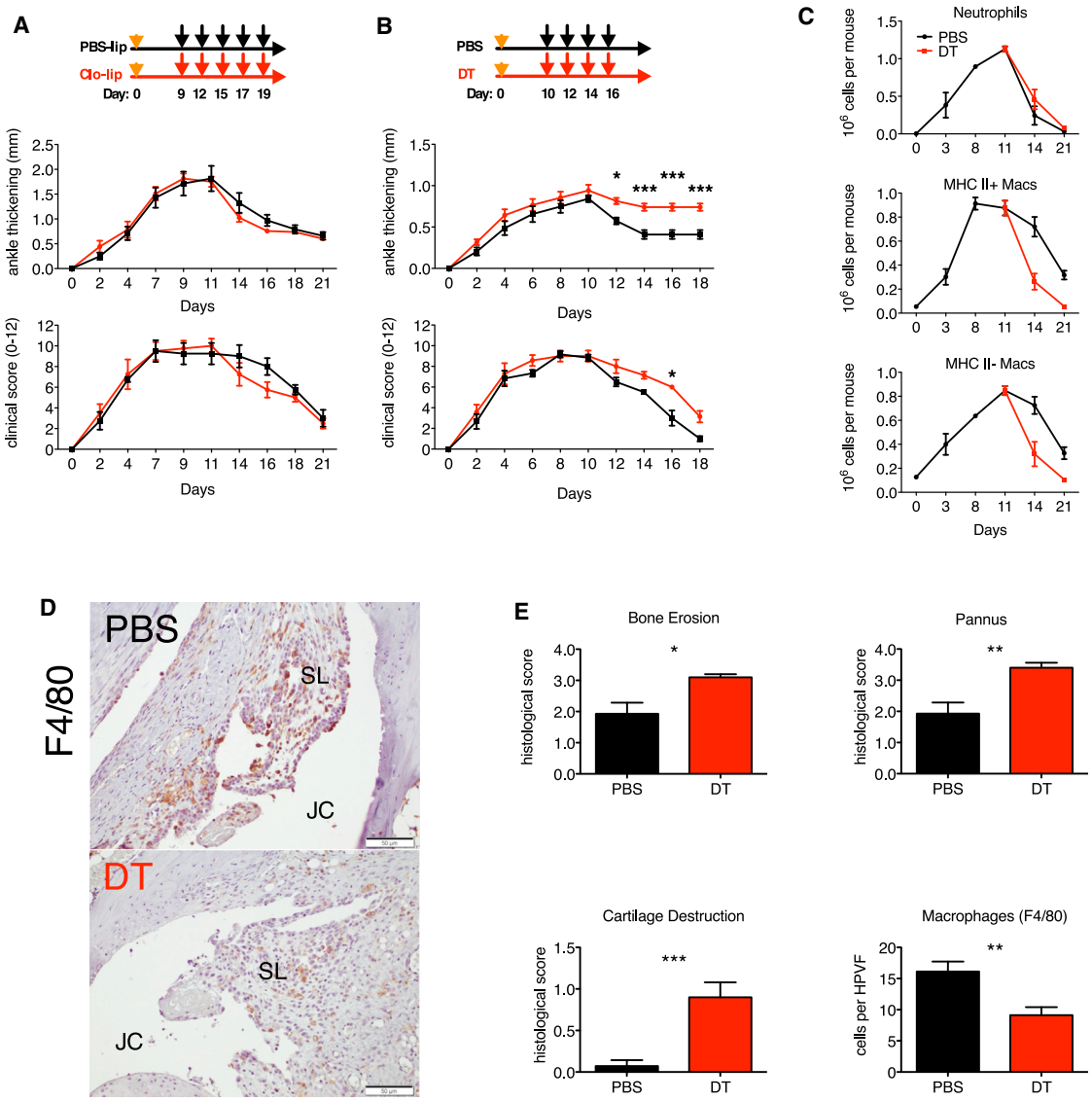

Figure 6. Role of Monocytes and Macrophages in the Resolution of STIA

(A) Depletion of monocytes does not affect resolution of STIA (n = 4).

(B) Depletion of monocytes and tissue macrophages during the resolution phase of STIA delays resolution of arthritis (n = 7).

(C) Repeated administration of DT depletes tissue macrophages.

(D) Repeated administration of DT depletes tissue macrophages: Immunohistochemistry was performed on ankle section for F4/80. The scale bar represents 50 μm.

(E) Depletion of tissue macrophages during resolution phase results in higher histopathological scores.

Data are represented as mean ± SEM. Differences between groups were compared using two-way ANOVA for repeated measurements with Bonferroni posttest (arthritis) or with Student's t test (histopathology); *p < 0.05; **p < 0.01; ***p < 0.001.

DISCUSSION

Synovial macrophages were discovered more than half a century ago and are known to be necessary for the development of arthritis (Barland et al., 1962); however, little is known about their origins and roles in maintenance of the normal joint or in the pathogenesis of RA. We used a strategy of depletion and selective rescue of nonclassical Ly6C$^-$ monocytes to show they are both necessary and sufficient for the initiation of STIA. Our data show that nonclassical Ly6C$^-$ monocytes can directly participate in tissue injury. Furthermore, our data suggest that the pathogenesis of autoimmune arthritis is distinct from other forms of tissue injury in which Ly6C$^+$ monocytes are preferentially recruited into inflamed tissues in a CCR2-dependent manner and give rise to inflammatory macrophages, as has been described during bacterial infection (Auffray et al., 2007; Serbina et al., 2003), myocardial infarction (Nahrendorf et al., 2007), muscle injury (Arnold et al., 2007), and CNS injury

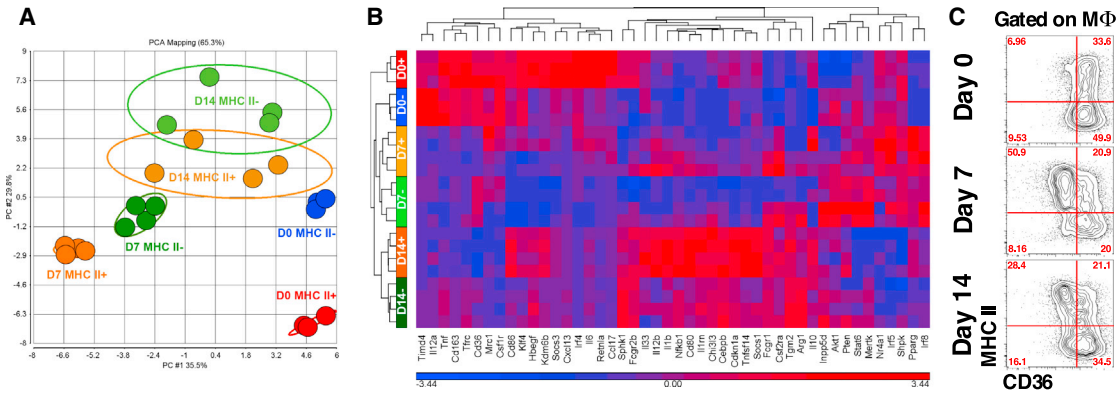

Figure 7. Synovial Macrophages Switch Phenotype during the Course of STIA

(A) Principal-component analysis of gene expression in synovial macrophages confirms the differential origins of MHC II$^+$ and MHC II$^-$ synovial macrophages in the steady state.

(B) Hierarchical clustering of 46 genes differentially expressed across the data set (FDR q value < 0.001).

(C) Expression of CD36 on synovial macrophages during the course of STIA and analyzed by flow cytometry. Representative contour plots are shown. Numbers represent percentages of the parent gate.

(Shechter et al., 2013). Our data explain the previous observation that *CCR2*$^{-/-}$ mice, which have decreased numbers of classical Ly6C$^+$ monocytes, develop the same magnitude of STIA as controls and have a similar ability to recruit monocytes into the joint. We describe an approach that can be used to determine whether nonclassical Ly6C$^-$ monocytes may contribute to tissue injury in other autoimmune models of inflammation as has been suggested (Mildner et al., 2013; Soehnlein and Lindbom, 2010). For example, in a model of autoimmune kidney injury, Carlin et al. (2013) suggested that nonclassical Ly6C$^-$ monocytes attract neutrophils in response to TLR7 stimulation and facilitate their extravasation into the tissue; however, they did not observe recruitment of nonclassical Ly6C$^-$ monocytes, possibly due to the short duration of observation. By selectively labeling only nonclassical Ly6C$^-$ monocytes, we were able to demonstrate that this monocyte subset is recruited into the joint during STIA, where they give rise to proinflammatory macrophages. Importantly, our strategy allowed us to follow the recruitment of nonclassical Ly6C$^-$ monocytes into the joint in the presence of classical Ly6C$^+$ monocytes. If a similar distinct role for nonclassical Ly6C$^-$ monocytes in the development of autoimmune inflammation in other models is confirmed, this would provide a new paradigm for understanding the molecular basis of these diseases.

Currently, there are no strategies in mice to selectively deplete nonclassical Ly6C$^-$ monocytes; however, their numbers are reduced in mice with deletions of *Cx3cr1*, *Nr4a1*, or *S1pr5* (Debien et al., 2013; Hanna et al., 2011; Landsman et al., 2009). Whereas the impact of NR4A1 or S1PR5 deficiency on STIA has not been studied, mice lacking CX_3CR1 have been reported to develop less STIA (Jacobs et al., 2010). Our data, in which even the adoptive transfer of a small number of nonclassical Ly6C$^-$ monocytes was sufficient to induce STIA, highlight the importance of this subset. Therefore, whereas our study does not dismiss the important role of neutrophils and classical Ly6C$^+$ monocytes in STIA, it clearly demonstrates that nonclassical Ly6C$^-$ monocytes are both necessary and sufficient for the initiation and propagation phases of arthritis.

The cellular composition of various macrophage populations in the naive and inflamed joint has been largely unexplored. Flow cytometric analysis extending beyond assessment of CD11b or Gr-1 expression has only been reported in rats (Moghaddami et al., 2005a, 2005b, 2007) or synovial fluid of knee joints (Bruhns et al., 2003). None of these studies included techniques that determined the origin of synovial macrophages. Here, we generated bone marrow chimeric mice with selective shielding of the joint during irradiation to demonstrate that the naive mouse joint contains a heterogeneous population of macrophages, namely tissue-resident and bone-marrow-derived macrophages (Ginhoux and Jung, 2014; Hashimoto et al., 2013; Yona et al., 2013). In the naive joint, the vast majority of the tissue-resident synovial macrophages are MHC II$^-$, whereas the bone-marrow-derived macrophages are mostly MHC II$^+$. Tissue-resident macrophages populate the synovial tissue early during embryonic development and are derived from outside of the bone marrow via a process that requires M-CSF. If M-CSF is absent during early embryogenesis, the synovium is populated with bone-marrow-derived macrophages, which may be recruited via interleukin (IL)-34, an alternative ligand for M-CSF-R (Wei et al., 2010). We found that depletion of tissue-resident MHC II$^-$ macrophages results in worsened STIA, suggesting these cells play an important role in maintaining tissue integrity and limiting inflammation (Lavin and Merad, 2013). We also show that tissue-resident macrophages exhibit a low level of proliferation during steady-state conditions and in inflammation. This local proliferation likely contributes to maintaining the population of tissue-resident macrophages during steady-state conditions; however, unlike other models of inflammation (Davies et al., 2011; Jenkins et al., 2011), it does not contribute to the increased number of synovial macrophages during STIA, a large majority of which are monocyte derived. This leaves open the possibility that inefficient repair mediated by tissue-resident macrophages may play a role in chronic arthritis. Unlike

tissue-resident macrophages, bone-marrow-derived macrophages are short lived and require constant influx of monocytes to maintain their population. Our short-term cell-tracking studies suggest that bone-marrow-derived monocytes do not contribute to the synovial macrophage population under steady-state conditions. However, in the absence of CCR2, Ly6C$^+$ monocytes can give rise to Ly6C$^+$CD64^{int} cells, which may differentiate into macrophages. The Ly6C$^+$CD64^{int} cells are not depleted after the systemic administration of clodronate-loaded liposomes, suggesting these cells may originate from extravasated tissue-surveying monocytes (Jakubzick et al., 2013).

Recently, macrophage polarization in health and disease has received a great deal of attention due to the therapeutic potential of altering macrophage phenotype. Macrophages may be readily manipulated in vitro to generate distinct classically activated/M1 or alternatively activated/M2 cells (Mosser and Edwards, 2008); however, their phenotypes in vivo may not be as straightforward (Sica and Mantovani, 2012; Xue et al., 2014). M1/M2 activation of synovial macrophages in STIA was dramatically different from M1 and M2 phenotypes obtained in vitro using lipopolysaccharide/interferon-γ or IL-4, correspondingly (data not shown). For example, inducible nitric oxide synthase, a hallmark of in vitro M1 activation, is not elevated at the peak of STIA. Similarly, *Mrc1* (CD206), *Retnla* (RELMα), and *Chi3l3* (Ym1) are not upregulated during the resolution phase. Instead, the resolution phase of STIA is associated with increased expression of genes involved in uptake of apoptotic debris and processing lipids, such as *Pparg* (PPARγ), *Mertk* (MerTK), *Tgm2* (Tgm2), and *Cd36* (CD36). The fact that subpopulations of synovial macrophages during the steady state and STIA exhibit mixed M1/M2 activation and differential expression of CD36 may suggest they are more heterogeneous than our current grouping based on expression of MHC II. Importantly, our findings of macrophage heterogeneity in mice are relevant to humans, as we observed a similar phenomenon using synovial biopsies from healthy volunteers and patients with RA. New technologies, such as parallel single-cell RNA sequencing (Jaitin et al., 2014), have the potential to allow unbiased analysis of the change in macrophage phenotype using animal models of RA and synovial tissue.

Whereas our labeling studies indicate that monocyte recruitment into the joints is continuous through all the phases of STIA, selective depletion of blood monocytes versus recruited macrophages confirms that the recruited macrophages are necessary for the resolution of arthritis and healing of the joint. These data show that the same classically activated macrophages recruited during the development of STIA phase switch their phenotype and become wound healing macrophages, and unlike in other models of inflammation, this process does not require the entrance of a second wave of monocytes into the tissue (Arnold et al., 2007; Nahrendorf et al., 2007; Shechter et al., 2009). This change in macrophage phenotype coincides with an upregulation of the molecules involved in efferocytosis and the rapid decrease in neutrophils from the joint, suggesting that apoptotic neutrophils into the joint during STIA may drive recruited macrophages toward a more M2 phenotype. This hypothesis is supported by findings in other models of tissue injury (Korns et al., 2011; Soehnlein and Lindbom, 2010). Whereas the systemic injection of apoptotic cells is not sufficient to prevent STIA (Gray et al., 2007), it is possible that phagocytosis of the apoptotic cells in the synovium may be more important for altering synovial macrophage phenotype than efferocytosis of apoptotic cells in the circulation. Consistent with this hypothesis, classically activated M1 macrophages recruited during early stages of STIA-mediated inflammation may efficiently clear apoptotic neutrophils (Korns et al., 2011).

In summary, we have identified a previously unrecognized role for nonclassical Ly6C$^-$ monocytes and tissue-resident macrophages in the development of autoimmune arthritis. Our data support a model in which Ly6C$^-$ nonclassical monocytes are recruited to the joint during inflammation, where they are both required and sufficient for the development of arthritis. Over the course of STIA, these same recruited macrophages undergo a remarkable change in their pattern of gene expression, initially expressing a complex set of both M1 and M2 genes followed by a shift toward a more M2 phenotype. This change in gene expression is accompanied by an alteration in function, as depletion of these macrophages at the peak of arthritis slows arthritis resolution. Throughout the course of STIA, tissue-resident synovial macrophages remain polarized toward a M2 phenotype and attenuate the severity of arthritis; however, their protective signals are likely overwhelmed by a relatively large influx of nonclassical monocytes from the circulation. Whether this mechanism may be generalized to other forms of autoimmune inflammation in other tissues warrants further investigation. The approach we have developed demonstrates how a better longitudinal understanding of the roles of individual subsets of monocytes, tissue macrophages, and neutrophils over the course of inflammation and its resolution can pave the way for improved strategies for targeting mononuclear phagocytes in autoimmune inflammation.

EXPERIMENTAL PROCEDURES

Mice

The following mouse strains were used: C57Bl/6, B6.SJL-*Ptprc*^{a} *Pepc*^{b}/BoyJ (CD45.1), *CCR2*$^{-/-}$, *Cx3cr1*$^{gfp/+}$ (Jung et al., 2000), B6.Cg-*Gt*(*ROSA*)*26Sor*$^{tm6(CAG-ZsGreen1)Hze}$/J; B6;C3Fe a/a-Csf1^{op}/J (*Csf1*^{op}), B6.FVB-Tg (ITGAM-DTR/EGFP)34Lan/J (CD11b-DTR), and B6.FVB-Tg(Itgax-DTR/EGFP)57Lan/J (CD11c-DTR). All mice were purchased from the Jackson Laboratory and bred and housed at a barrier and specific pathogen-free facility at the Center for Comparative Medicine at Northwestern University. Eight- to ten-week-old mice were used for all experiments. All procedures were approved by the Institutional Animal Care and Use committee at Northwestern University. Generation of CD11b-DTR and CD11c-DTR bone marrow chimeras, diphtheria toxin treatment, and monocyte depletion are described in Supplemental Experimental Procedures.

K/BxN Serum-Transfer-Induced Arthritis

Serum transfer arthritis was induced by intravenous injection of 75 μl of arthritogenic serum from 8-week-old progeny of KRN and nonobese diabetic (NOD) mice (K/BxN) mice (Monach et al., 2008). Change in ankle thickness was monitored using caliper (Fowler Tools of Canada). In addition, clinical score was assessed as a sum of the clinical score for each paw (0, no arthritis; 1, mild arthritis, foot maintains V-shape; 2, moderate arthritis, foot no longer maintains V-shape; 3, severe arthritis). Each experiment was performed two to five times to confirm reproducibility. Whenever possible, scoring was performed in a blinded manner. Histological and histopathological assessment of arthritis is described in Supplemental Experimental Procedures.

Tissue Preparation and Flow Cytometry

Blood was collected into EDTA-containing tubes either via facial vein bleed (from live animals) or via cardiac puncture (from euthanized animals). Whole blood was stained with fluorochrome-conjugated antibodies, and erythrocytes were then lysed using BD FACS lysing solution (BD Biosciences). Spleen was digested using mixture of Collagenase D and DNase I (both from Roche) in Hank's balanced salt solution (HBSS) at 37°C for 30 min and filtered through 40 μm nylon mesh. Erythrocytes were lysed using BD Pharm Lyse (BD Biosciences), and cells were counted using Countess automated cell counter (Invitrogen); dead cells were discriminated using trypan blue. For ankle analysis, mice were perfused through the left ventricle with 20 ml of HBSS. Ankles were cut 3 mm above the heel, and skin from the feet was removed. To avoid contamination with the bone marrow, bone marrow cavity in the tibia was thoroughly flushed with HBSS, fingers were disarticulated by pulling with blunt forceps, and tibiotalar joint was opened via posterior access route to expose synovial lining. The foot was incubated in digestion buffer (2 mg/ml dispase II, 2 mg/ml collagenase D, and 1 mg/ml of DNase I in HBSS) for 60 min at 37°C. Cells released during the digestion were filtered through 40 μm nylon mesh, erythrocytes were lysed using BD Pharm Lyse (BD Biosciences), and cells were counted using Countess automated cell counter (Invitrogen); dead cells were discriminated using trypan blue. Cells were stained with live/dead Aqua (Invitrogen) or eFluor 506 (eBioscience) viability dyes, incubated with FcBlock (BD Bioscience), and stained with fluorochrome-conjugated antibodies (see Table S1 for the list of antibodies, clones, fluorochromes, and manufacturers). Data were acquired on BD LSR II flow cytometer (BD Biosciences; see Table S2 for instrument configuration). Compensation and analysis of the flow cytometry data were performed using FlowJo software (Tree Star). "Fluorescence minus one" controls were used when necessary to set up gates. Expression of the activation markers presented as median fluorescence intensity. Click-iT EdU Kit (Invitrogen) was used to assess the macrophage proliferation. Cell sorting was performed at University of Chicago Flow Cytometry core facility and at Northwestern University Robert H. Lurie Comprehensive Cancer Center Flow Cytometry core facility on FACSAria III instrument (BD Biosciences) with the same configuration as LSR II. Cytospins were prepared from sorted cells and stained with Diff-Quik Stain Set (Siemens Healthcare). Microphotographs of the individual representative cells were taken on Nikon Eclipse TE2000E2 microscope, and representative images of the individual cells were combined into one panel using Adobe Photoshop without any additional manipulations.

Analysis of Macrophage Polarization

Synovial macrophages from steady-state or STIA ankles were sorted using FACSAria III instrument, washed once, and cell pellets were lysed directly in QuantiGene Cell Lysis Mixture. Gene-expression profiles were determined using custom QuantiGene 2.0 assay (panel no. 21522; Affymetrix) on Luminex 200 instrument (Luminex); see Table S4 for the panel description. Data were normalized to expression of housekeeping genes and imported into Partek Genomics Suite V6.6 software (Partek). Differentially expressed genes between the different groups of macrophages as well as transcripts with variable expression within the data set were calculated using one-way ANOVA. Differentially expressed genes were defined by a fold change greater than 1.4 and a FDR-corrected q-value < 0.001 unless stated otherwise. Principle-component analysis using all transcripts was used for visualization of sample relationships. Hierarchical clustering of the differentially expressed genes was performed based on Euclidean algorithm for dissimilarity and average linkage method to determine distance between clusters.

Statistical Analysis

In arthritis experiments, differences in ankle width and clinical score between the groups were assessed using two-way ANOVA for repeated measurements with Bonferroni posttest to compare differences between the groups. For histopathological scores, differences between groups were determined using Student's t tests. All analyses were performed using GraphPad Prism version 5.00 (GraphPad Software). Data are shown as means ± SEM unless stated otherwise.

Additional materials and methods can be found in Supplemental Information.

SUPPLEMENTAL INFORMATION

Supplemental Information includes Supplemental Experimental Procedures, four figures, and five tables and can be found with this article online at http://dx.doi.org/10.1016/j.celrep.2014.09.032.

ACKNOWLEDGMENTS

Northwestern University Cell Imaging Facility and Flow Cytometry Core Facility are supported by NCI Cancer Center Support Grant CA060553 awarded to the Robert H. Lurie Comprehensive Cancer Center. This work was supported by NIH grants AR050250, AR054796, AR064546, AI092490, and HL108795 and funds provided by United States-Israel Binational Science Foundation (2013247), Rheumatology Research Foundation (Agmt 05/06/14), Solovy/Arthritis Research Society, and Arthritis Research UK (grant 18547). We thank Dr. Steffen Jung for providing us with MC-21 antibody. We also thank Drs. Christian Stehlik, Navdeep Chandel, and Richard M. Pope for their critical evaluation of the manuscript and valuable comments.

Received: January 17, 2014
Revised: August 5, 2014
Accepted: September 17, 2014
Published: October 16, 2014

REFERENCES

Arnold, L., Henry, A., Poron, F., Baba-Amer, Y., van Rooijen, N., Plonquet, A., Gherardi, R.K., and Chazaud, B. (2007). Inflammatory monocytes recruited after skeletal muscle injury switch into antiinflammatory macrophages to support myogenesis. J. Exp. Med. *204*, 1057–1069.

Auffray, C., Fogg, D., Garfa, M., Elain, G., Join-Lambert, O., Kayal, S., Sarnacki, S., Cumano, A., Lauvau, G., and Geissmann, F. (2007). Monitoring of blood vessels and tissues by a population of monocytes with patrolling behavior. Science *317*, 666–670.

Auffray, C., Sieweke, M.H., and Geissmann, F. (2009). Blood monocytes: development, heterogeneity, and relationship with dendritic cells. Annu. Rev. Immunol. *27*, 669–692.

Barland, P., Novikoff, A.B., and Hamerman, D. (1962). Electron microscopy of the human synovial membrane. J. Cell Biol. *14*, 207–220.

Bruhns, P., Samuelsson, A., Pollard, J.W., and Ravetch, J.V. (2003). Colony-stimulating factor-1-dependent macrophages are responsible for IVIG protection in antibody-induced autoimmune disease. Immunity *18*, 573–581.

Cailhier, J.F., Sawatzky, D.A., Kipari, T., Houlberg, K., Walbaum, D., Watson, S., Lang, R.A., Clay, S., Kluth, D., Savill, J., and Hughes, J. (2006). Resident pleural macrophages are key orchestrators of neutrophil recruitment in pleural inflammation. Am. J. Respir. Crit. Care Med. *173*, 540–547.

Carlin, L.M., Stamatiades, E.G., Auffray, C., Hanna, R.N., Glover, L., Vizcay-Barrena, G., Hedrick, C.C., Cook, H.T., Diebold, S., and Geissmann, F. (2013). Nr4a1-dependent Ly6C(low) monocytes monitor endothelial cells and orchestrate their disposal. Cell *153*, 362–375.

Davies, L.C., Rosas, M., Smith, P.J., Fraser, D.J., Jones, S.A., and Taylor, P.R. (2011). A quantifiable proliferative burst of tissue macrophages restores homeostatic macrophage populations after acute inflammation. Eur. J. Immunol. *41*, 2155–2164.

Davies, L.C., Jenkins, S.J., Allen, J.E., and Taylor, P.R. (2013a). Tissue-resident macrophages. Nat. Immunol. *14*, 986–995.

Davies, L.C., Rosas, M., Jenkins, S.J., Liao, C.T., Scurr, M.J., Brombacher, F., Fraser, D.J., Allen, J.E., Jones, S.A., and Taylor, P.R. (2013b). Distinct bone marrow-derived and tissue-resident macrophage lineages proliferate at key stages during inflammation. Nat. Commun. *4*, 1886.

Debien, E., Mayol, K., Biajoux, V., Daussy, C., De Aguero, M.G., Taillardet, M., Dagany, N., Brinza, L., Henry, T., Dubois, B., et al. (2013). S1PR5 is pivotal for the homeostasis of patrolling monocytes. Eur. J. Immunol. *43*, 1667–1675.

Gautier, E.L., Shay, T., Miller, J., Greter, M., Jakubzick, C., Ivanov, S., Helft, J., Chow, A., Elpek, K.G., Gordonov, S., et al.; Immunological Genome Consortium (2012). Gene-expression profiles and transcriptional regulatory pathways that underlie the identity and diversity of mouse tissue macrophages. Nat. Immunol. *13*, 1118–1128.

Ginhoux, F., and Jung, S. (2014). Monocytes and macrophages: developmental pathways and tissue homeostasis. Nat. Rev. Immunol. *14*, 392–404.

Ginhoux, F., Greter, M., Leboeuf, M., Nandi, S., See, P., Gokhan, S., Mehler, M.F., Conway, S.J., Ng, L.G., Stanley, E.R., et al. (2010). Fate mapping analysis reveals that adult microglia derive from primitive macrophages. Science *330*, 841–845.

Gray, M., Miles, K., Salter, D., Gray, D., and Savill, J. (2007). Apoptotic cells protect mice from autoimmune inflammation by the induction of regulatory B cells. Proc. Natl. Acad. Sci. USA *104*, 14080–14085.

Hamers, A.A., Vos, M., Rassam, F., Marinković, G., Kurakula, K., van Gorp, P.J., de Winther, M.P., Gijbels, M.J., de Waard, V., and de Vries, C.J. (2012). Bone marrow-specific deficiency of nuclear receptor Nur77 enhances atherosclerosis. Circ. Res. *110*, 428–438.

Hanna, R.N., Carlin, L.M., Hubbeling, H.G., Nackiewicz, D., Green, A.M., Punt, J.A., Geissmann, F., and Hedrick, C.C. (2011). The transcription factor NR4A1 (Nur77) controls bone marrow differentiation and the survival of Ly6C- monocytes. Nat. Immunol. *12*, 778–785.

Hanna, R.N., Shaked, I., Hubbeling, H.G., Punt, J.A., Wu, R., Herrley, E., Zaugg, C., Pei, H., Geissmann, F., Ley, K., and Hedrick, C.C. (2012). NR4A1 (Nur77) deletion polarizes macrophages toward an inflammatory phenotype and increases atherosclerosis. Circ. Res. *110*, 416–427.

Haringman, J.J., Gerlag, D.M., Zwinderman, A.H., Smeets, T.J., Kraan, M.C., Baeten, D., McInnes, I.B., Bresnihan, B., and Tak, P.P. (2005). Synovial tissue macrophages: a sensitive biomarker for response to treatment in patients with rheumatoid arthritis. Ann. Rheum. Dis. *64*, 834–838.

Hashimoto, D., Chow, A., Noizat, C., Teo, P., Beasley, M.B., Leboeuf, M., Becker, C.D., See, P., Price, J., Lucas, D., et al. (2013). Tissue-resident macrophages self-maintain locally throughout adult life with minimal contribution from circulating monocytes. Immunity *38*, 792–804.

Helmick, C.G., Felson, D.T., Lawrence, R.C., Gabriel, S., Hirsch, R., Kwoh, C.K., Liang, M.H., Kremers, H.M., Mayes, M.D., Merkel, P.A., et al.; National Arthritis Data Workgroup (2008). Estimates of the prevalence of arthritis and other rheumatic conditions in the United States. Part I. Arthritis Rheum. *58*, 15–25.

Jacobs, J.P., Ortiz-Lopez, A., Campbell, J.J., Gerard, C.J., Mathis, D., and Benoist, C. (2010). Deficiency of CXCR2, but not other chemokine receptors, attenuates autoantibody-mediated arthritis in a murine model. Arthritis Rheum. *62*, 1921–1932.

Jaitin, D.A., Kenigsberg, E., Keren-Shaul, H., Elefant, N., Paul, F., Zaretsky, I., Mildner, A., Cohen, N., Jung, S., Tanay, A., and Amit, I. (2014). Massively parallel single-cell RNA-seq for marker-free decomposition of tissues into cell types. Science *343*, 776–779.

Jakubzick, C., Gautier, E.L., Gibbings, S.L., Sojka, D.K., Schlitzer, A., Johnson, T.E., Ivanov, S., Duan, Q., Bala, S., Condon, T., et al. (2013). Minimal differentiation of classical monocytes as they survey steady-state tissues and transport antigen to lymph nodes. Immunity *39*, 599–610.

Jenkins, S.J., Ruckerl, D., Cook, P.C., Jones, L.H., Finkelman, F.D., van Rooijen, N., MacDonald, A.S., and Allen, J.E. (2011). Local macrophage proliferation, rather than recruitment from the blood, is a signature of TH2 inflammation. Science *332*, 1284–1288.

Jung, S., Aliberti, J., Graemmel, P., Sunshine, M.J., Kreutzberg, G.W., Sher, A., and Littman, D.R. (2000). Analysis of fractalkine receptor CX(3)CR1 function by targeted deletion and green fluorescent protein reporter gene insertion. Mol. Cell. Biol. *20*, 4106–4114.

Kawanaka, N., Yamamura, M., Aita, T., Morita, Y., Okamoto, A., Kawashima, M., Iwahashi, M., Ueno, A., Ohmoto, Y., and Makino, H. (2002). CD14+,CD16+ blood monocytes and joint inflammation in rheumatoid arthritis. Arthritis Rheum. *46*, 2578–2586.

Kinne, R.W., Stuhlmüller, B., and Burmester, G.R. (2007). Cells of the synovium in rheumatoid arthritis. Macrophages. Arthritis Res. Ther. *9*, 224.

Korns, D., Frasch, S.C., Fernandez-Boyanapalli, R., Henson, P.M., and Bratton, D.L. (2011). Modulation of macrophage efferocytosis in inflammation. Front. Immunol. *2*, 57.

Landsman, L., Bar-On, L., Zernecke, A., Kim, K.W., Krauthgamer, R., Shagdarsuren, E., Lira, S.A., Weissman, I.L., Weber, C., and Jung, S. (2009). CX3CR1 is required for monocyte homeostasis and atherogenesis by promoting cell survival. Blood *113*, 963–972.

Lavin, Y., and Merad, M. (2013). Macrophages: gatekeepers of tissue integrity. Cancer Immunol. Res. *1*, 201–209.

Lech, M., and Anders, H.J. (2013). Macrophages and fibrosis: How resident and infiltrating mononuclear phagocytes orchestrate all phases of tissue injury and repair. Biochim. Biophys. Acta *1832*, 989–997.

Lichanska, A.M., Browne, C.M., Henkel, G.W., Murphy, K.M., Ostrowski, M.C., McKercher, S.R., Maki, R.A., and Hume, D.A. (1999). Differentiation of the mononuclear phagocyte system during mouse embryogenesis: the role of transcription factor PU.1. Blood *94*, 127–138.

Maus, U.A., Koay, M.A., Delbeck, T., Mack, M., Ermert, M., Ermert, L., Blackwell, T.S., Christman, J.W., Schlöndorff, D., Seeger, W., and Lohmeyer, J. (2002). Role of resident alveolar macrophages in leukocyte traffic into the alveolar air space of intact mice. Am. J. Physiol. Lung Cell. Mol. Physiol. *282*, L1245–L1252.

Mildner, A., Yona, S., and Jung, S. (2013). A close encounter of the third kind: monocyte-derived cells. Adv. Immunol. *120*, 69–103.

Moghaddami, M., Cleland, L.G., and Mayrhofer, G. (2005a). MHC II+ CD45+ cells from synovium-rich tissues of normal rats: phenotype, comparison with macrophage and dendritic cell lineages and differentiation into mature dendritic cells in vitro. Int. Immunol. *17*, 1103–1115.

Moghaddami, M., Mayrhofer, G., and Cleland, L.G. (2005b). MHC class II compartment, endocytosis and phagocytic activity of macrophages and putative dendritic cells isolated from normal tissues rich in synovium. Int. Immunol. *17*, 1117–1130.

Moghaddami, M., Cleland, L.G., Radisic, G., and Mayrhofer, G. (2007). Recruitment of dendritic cells and macrophages during T cell-mediated synovial inflammation. Arthritis Res. Ther. *9*, R120.

Monach, P.A., Mathis, D., and Benoist, C. (2008). The K/BxN arthritis model. Curr. Protoc. Immunol. *Chapter 15*, Unit 15.22.

Mosser, D.M., and Edwards, J.P. (2008). Exploring the full spectrum of macrophage activation. Nat. Rev. Immunol. *8*, 958–969.

Mulherin, D., Fitzgerald, O., and Bresnihan, B. (1996). Synovial tissue macrophage populations and articular damage in rheumatoid arthritis. Arthritis Rheum. *39*, 115–124.

Nahrendorf, M., Swirski, F.K., Aikawa, E., Stangenberg, L., Wurdinger, T., Figueiredo, J.L., Libby, P., Weissleder, R., and Pittet, M.J. (2007). The healing myocardium sequentially mobilizes two monocyte subsets with divergent and complementary functions. J. Exp. Med. *204*, 3037–3047.

Schulz, C., Gomez Perdiguero, E., Chorro, L., Szabo-Rogers, H., Cagnard, N., Kierdorf, K., Prinz, M., Wu, B., Jacobsen, S.E., Pollard, J.W., et al. (2012). A lineage of myeloid cells independent of Myb and hematopoietic stem cells. Science *336*, 86–90.

Serbina, N.V., Salazar-Mather, T.P., Biron, C.A., Kuziel, W.A., and Pamer, E.G. (2003). TNF/iNOS-producing dendritic cells mediate innate immune defense against bacterial infection. Immunity *19*, 59–70.

Shechter, R., London, A., Varol, C., Raposo, C., Cusimano, M., Yovel, G., Rolls, A., Mack, M., Pluchino, S., Martino, G., et al. (2009). Infiltrating blood-derived macrophages are vital cells playing an anti-inflammatory role in recovery from spinal cord injury in mice. PLoS Med. *6*, e1000113.

Shechter, R., Miller, O., Yovel, G., Rosenzweig, N., London, A., Ruckh, J., Kim, K.W., Klein, E., Kalchenko, V., Bendel, P., et al. (2013). Recruitment of beneficial M2 macrophages to injured spinal cord is orchestrated by remote brain choroid plexus. Immunity *38*, 555–569.

Sica, A., and Mantovani, A. (2012). Macrophage plasticity and polarization: in vivo veritas. J. Clin. Invest. *122*, 787–795.

Soehnlein, O., and Lindbom, L. (2010). Phagocyte partnership during the onset and resolution of inflammation. Nat. Rev. Immunol. *10*, 427–439.

Stuhlmüller, B., Ungethüm, U., Scholze, S., Martinez, L., Backhaus, M., Kraetsch, H.G., Kinne, R.W., and Burmester, G.R. (2000). Identification of known and novel genes in activated monocytes from patients with rheumatoid arthritis. Arthritis Rheum. *43*, 775–790.

Torsteinsdóttir, I., Arvidson, N.G., Hällgren, R., and Håkansson, L. (1999). Monocyte activation in rheumatoid arthritis (RA): increased integrin, Fc gamma and complement receptor expression and the effect of glucocorticoids. Clin. Exp. Immunol. *115*, 554–560.

van Furth, R., and Cohn, Z.A. (1968). The origin and kinetics of mononuclear phagocytes. J. Exp. Med. *128*, 415–435.

Vincent, T.L., Williams, R.O., Maciewicz, R., Silman, A., and Garside, P.; Arthritis Research UK animal models working group (2012). Mapping pathogenesis of arthritis through small animal models. Rheumatology (Oxford) *51*, 1931–1941.

Wei, S., Nandi, S., Chitu, V., Yeung, Y.G., Yu, W., Huang, M., Williams, L.T., Lin, H., and Stanley, E.R. (2010). Functional overlap but differential expression of CSF-1 and IL-34 in their CSF-1 receptor-mediated regulation of myeloid cells. J. Leukoc. Biol. *88*, 495–505.

Xiong, W., Frasch, S.C., Thomas, S.M., Bratton, D.L., and Henson, P.M. (2013). Induction of TGF-β1 synthesis by macrophages in response to apoptotic cells requires activation of the scavenger receptor CD36. PLoS ONE *8*, e72772.

Xue, J., Schmidt, S.V., Sander, J., Draffehn, A., Krebs, W., Quester, I., De Nardo, D., Gohel, T.D., Emde, M., Schmidleithner, L., et al. (2014). Transcriptome-based network analysis reveals a spectrum model of human macrophage activation. Immunity *40*, 274–288.

Yona, S., Kim, K.W., Wolf, Y., Mildner, A., Varol, D., Breker, M., Strauss-Ayali, D., Viukov, S., Guilliams, M., Misharin, A., et al. (2013). Fate mapping reveals origins and dynamics of monocytes and tissue macrophages under homeostasis. Immunity *38*, 79–91.

Ziegler-Heitbrock, L., Ancuta, P., Crowe, S., Dalod, M., Grau, V., Hart, D.N., Leenen, P.J., Liu, Y.J., MacPherson, G., Randolph, G.J., et al. (2010). Nomenclature of monocytes and dendritic cells in blood. Blood *116*, e74–e80.